



*Journal of Geophysical Research-Solid Earth*

Supporting Information for

**Melt Segregation and Depletion during Ascent of Buoyant Diapirs in Subduction Zones**

Nan Zhang<sup>1,2,3</sup>, Mark D. Behn<sup>1</sup>, E. Marc Parmentier<sup>4</sup>, and Christopher Kincaid<sup>5</sup>

<sup>1</sup>Department of Geology & Geophysics, Woods Hole Oceanography Institution, Woods Hole, MA, USA

<sup>2</sup>Institution of Earth and Space Sciences, Peking University, China

<sup>3</sup>Department of Applied Geology, Curtin University, Australia

<sup>4</sup>Department of Earth, Environmental and Planetary Sciences, Brown University, Providence, RI, USA

<sup>5</sup>School of Oceanography, University of Rhode Island, RI

Corresponding author: [nan\\_zhang@pku.edu.cn](mailto:nan_zhang@pku.edu.cn)

**Contents of this file**

Text S1

Figures S1 and S2

Tables S1

**Additional Supporting Information (Files uploaded separately)**

Captions for Datasets S1 to S5

**Introduction**

The texts show a benchmark calculation for our two-phase flow code.

### **Text S1.**

#### **Solitary Wave Benchmark:**

The Darcy flow of melt, coupled with mantle convection, supports the emergence of non-linear solitary waves [See references in main article: *Scott & Stevenson*, 1984, 1986; *Richter & McKenzie*, 1984; *Barcilon & Richter*, 1986]. The incompressible solitary wave case has become a classic benchmark for examining magma migration codes. We tested our code with 1D solitary wave. In practice, we follow the parameters (Table S1) used in the solitary wave model by *Dannberg & Heister* [2016] (See references in main article). For a constant shear and compaction viscosities, the shape of the solitary wave can be described by an analytical solution

$$x(\varphi) = \pm(A + 0.5) \left[ -2\sqrt{A - \varphi} + \frac{1}{\sqrt{A-1}} \ln \frac{\sqrt{A-1}-\sqrt{A-\varphi}}{\sqrt{A-1}+\sqrt{A-\varphi}} \right] \quad (S1),$$

where  $A$  is the non-dimensional amplitude of the wave and bigger than 1 [See references in main article: *Barcilon & Richter*, 1986]. This equation describes a wave with the amplitude  $A\varphi_0$  propagating with a fixed shape and constant phase speed  $c = u_0(2A/\varphi_0+1)$  in a background porosity ( $\varphi=\varphi_0$ ). This background porosity is assumed to be small, i.e.,  $\varphi_0 \ll 1$ .

We consider a pseudo-1-D profile with a vertical length of 438 m but several elements in the horizontal direction, as our model geometry of 1-D solitary wave. The vertical length is chosen to be 128 times the compaction length. We vary our model resolution in the vertical direction based on the compaction length of 3.42 m (Table S1). We set the end time of the model to  $t = 2.643 \times 10^3$  kyrs to allow the wave to propagate 128 times the compaction length. Most of our parameters are taken from *Dannberg & Heister* [2016] (See references in main article) except for the resolution (Table S1). The phase velocity is set to be negative so that the wave is stationary at its origin position. Figure S1(A) displays the shape of the solitary wave after traveling 64 times compaction length, as well as the analytical solution.

We estimate our model accuracy by comparing the shape of the wave after the model runtime to this analytical solution (See references in main article: *Dannberg & Heister* [2016]). For this purpose, we calculate the deviation of the shape of the modelled wave from the analytical solution as

$$e_\varphi = \frac{\|\varphi_{num}(z+\Delta z) - \varphi_{ana}(z)\|_2}{A} \quad (S2),$$

where  $\varphi_{num}$  is our numerical solution,  $\varphi_{ana}$  is the 1D analytical solution, and  $\Delta z = c\Delta t$  is the phase shift.

Figure S1(B) demonstrates the evolution of this porosity error with spatial resolution of the compaction length. After an initial transient stage, the shape error remains constant. This shows that our code can capture the expected behavior of a solitary wave that moves with a constant phase speed without changing its shape. The errors decrease with increasing resolution, but saturate at a level of around 0.25 grid resolution (Figure S1(C)). The convergence becomes slower after the mesh size is less than the compaction length, as solitary waves are the solution of a simplified formulation of the porous flow equations that is only valid in the limit of small porosity.

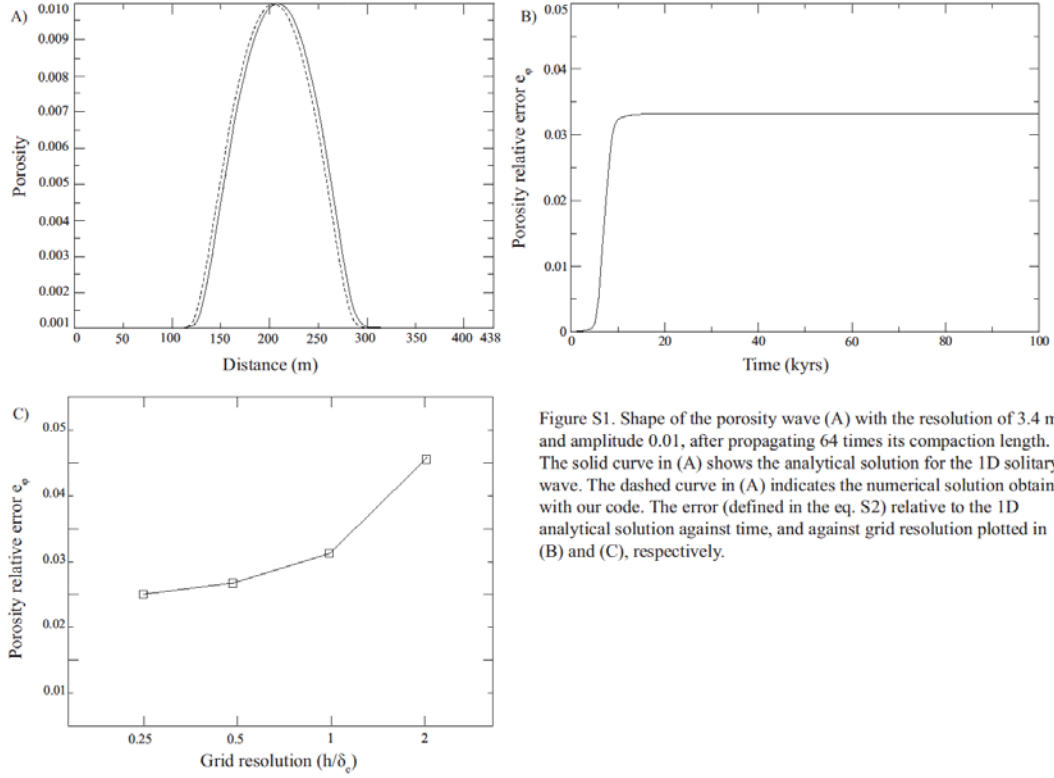
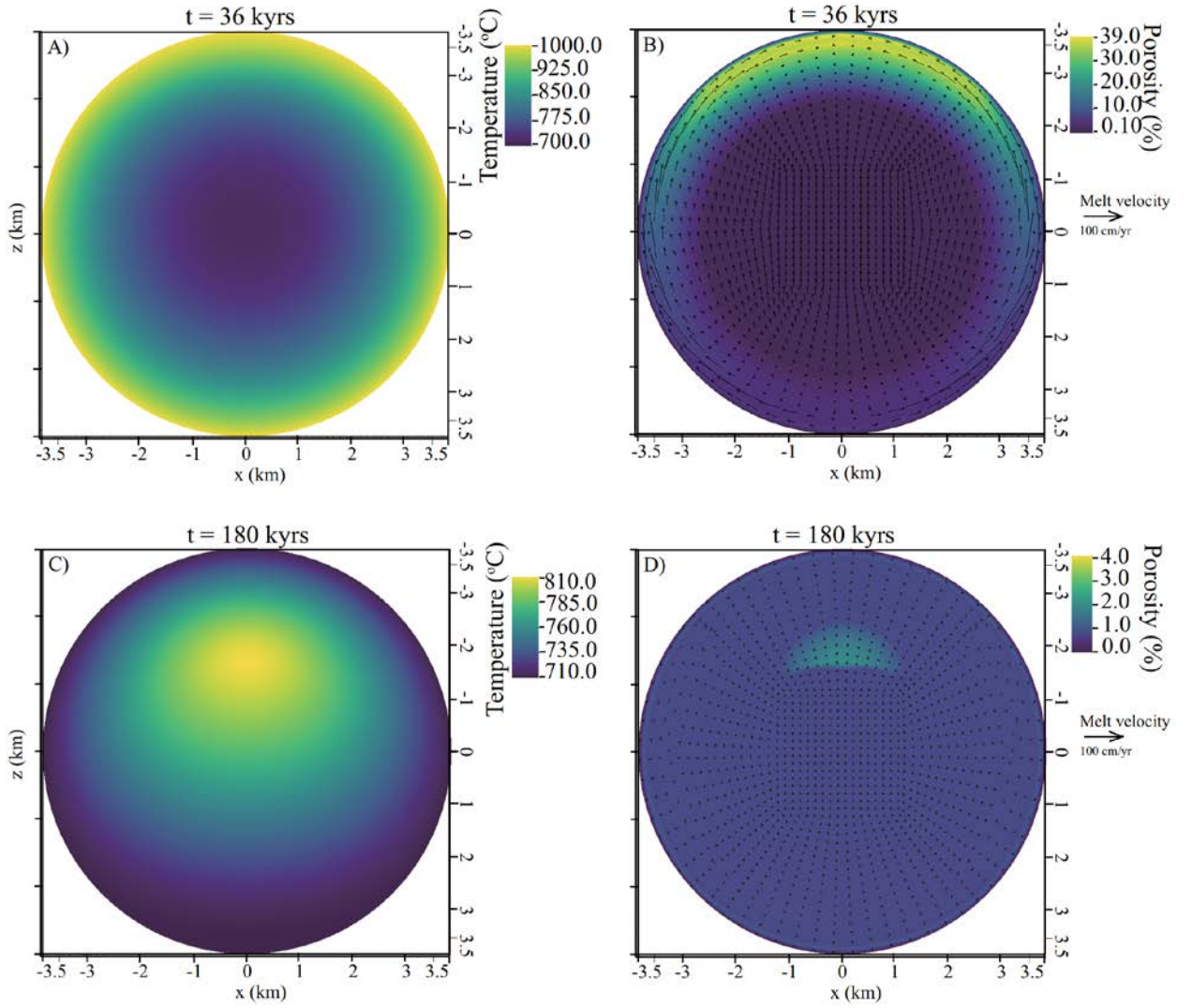


Figure S1. Shape of the porosity wave (A) with the resolution of 3.4 m and amplitude 0.01, after propagating 64 times its compaction length. The solid curve in (A) shows the analytical solution for the 1D solitary wave. The dashed curve in (A) indicates the numerical solution obtained with our code. The error (defined in the eq. S2) relative to the 1D analytical solution against time, and against grid resolution plotted in (B) and (C), respectively.

**Figure S1.** Shape of the porosity wave (A) with the resolution of 3.4 m and amplitude 0.01, after propagating 64 times its compaction length. The solid curve in (A) shows the analytical solution for the 1D solitary wave. The dashed curve in (A) indicates the numerical solution obtained with our code. The error (defined in the eq. S2) relative to the 1D analytical solution against time, and against grid resolution plotted in (B) and (C), respectively.



**Figure S2.** The temperature (A and C), and porosity and melt velocity (B and D) fields from the impermeable big diapir case CL12.8\_I\_R3.7.

Table S1. Parameters for the solitary wave benchmark.

Parameters	Value
Compaction length, $\delta_c$	3.42 m
Phase speed, $c$	$1.66 \times 10^{-4} \text{ m/yr}$
Solid matrix density, $\rho_s$	$3000 \text{ kg.m}^{-3}$
Melt density, $\rho_f$	$2500 \text{ kg.m}^{-3}$
Reference permeability, $K_0$	$5 \times 10^{-18} \text{ m}^2$
Reference porosity, $\phi_0$	$10^{-3}$
Shear viscosity of solid matrix, $\eta_0$	$10^{20} \text{ Pa.s}$
Melt viscosity, $\mu$	$100 \text{ Pa.s}$
Bulk viscosity, $\zeta$	$10^{20} \text{ Pa.s}$
Gravitational acceleration, $g$	$10 \text{ m/s}^2$
Reference velocity, $u_0$	$2.5 \times 10^{-13} \text{ m s}^{-1}$
Vertical grids number, $n_z$	64,128,256, 512
Resolution, $h$	6.84, 3.42, 1.71, 0.855 m

**Captions for Datasets S1 to S5:**

Dataset S1: The matlab script to produce the Fig.1B.

Dataset S2: The matlab script to reproduce the trajectory.

Dataset S3: The data file for the mantle wedge thermal structure and matlab script to plot it.

Dataset S4: The temperature-pressure-time determination. Combining S2 and S3, the T-P-t trajectory is obtained.

Dataset S5: The source code for the case of the impermeable large diapir. This source code is based on deal.ii libraries; installation information can be found at (<https://dealii.org/9.0.0/index.html>).